Velocity component and diameter distribution characteristics of droplets within two interacting electrohydrodynamic sprays

Patrick F. Dunn and Stephen R. Snarski
Department of Aerospace and Mechanical Engineering, University of Notre Dame, Notre Dame, Indiana 46556

(Received 2 April 1990; accepted 5 November 1990)

The droplet axial and lateral velocity distributions, diameter distributions, and velocity-component–diameter correlations in the interaction region of two sprays of electrically charged, micrometer-sized droplets are presented and discussed. These results reveal the occurrence of interspray droplet mixing and a correlation between velocity component and diameter within the mixing region. They further support that interspray droplet mixing and the evolution toward a spatially uniform combined spray are enhanced with increasing spray charge density and decreasing interneedle spacing.

This Brief Communication addresses several outstanding issues concerning the interaction that occurs between the charged droplets of two adjacent, electrohydrodynamic (EHD) sprays. Herein, we present the effect of spray charge density, which has been shown by Kelly[1] to be the essential correlating parameter of an EHD spray, on the mean droplet sizes and velocity components. Further, we examine the extent of the velocity-component–diameter correlations of the two sprays and provide evidence for the occurrence of interspray droplet mixing.

The data considered are those reported by Snarski and Dunn[2] of droplet axial and lateral velocity components and diameter obtained using a phase Doppler particle analyzer (Bachalo and Houser[3]). Two sprays of droplets in the approximate diameter range of 1–50 μm were generated electrohydrodynamically in those experiments by supplying ethanol at a fixed mass flow rate (4.5 mg/sec per needle) and applying a high positive voltage to two adjacent hypodermic needles (216 μm i.d., 406 μm o.d., 1.905 cm length) located 38 cm above an electrically grounded droplet-collection funnel. Data were acquired at two axial positions below the needles' tips (15 and 30 mm) for two interneedle spacings (1 and 3 cm) and at four applied voltages (15, 20, 25, and 30 kV). These voltages corresponded to average spray charge densities of 59, 116, 184, and 278 C/m^3, respectively.

Cross-sectional averages (csa's) can be computed from the mean velocity component and Sauter mean diameter profiles across the lateral span of the sprays to illustrate the overall effect of increasing spray charge density. As shown in Fig. 1, for the 3 cm interneedle spacing, both velocity components increase in magnitude with increasing spray charge density and are insensitive to axial position. (Similar trends were observed for both spacings.) The csa axial velocity components, however, exhibit much greater sensitivity to changes in spray charge density than their lateral counterparts, as evidenced by their greater slope, and are approximately twice their magnitude at all spray charge densities. Also there is a net decrease in the csa Sauter mean diameter with increasing spray charge densities, with that diameter asymptotically approaching a constant value (approximately to within experimental error) at a charge density of 184 C/m^3, independent of axial position.

Detail on the spatial dispersion of the droplets is revealed in the axial and lateral velocity and diameter distributions at several locations within the sprays. Here, only the results of 278 C/m^3, at which the most interaction between the two sprays occurred, are presented. The axial and lateral velocity and diameter distributions, obtained at an interneedle spacing of 1 cm and a distance of 15 mm below the plane of the needles' tips, are shown in Fig. 2, for three representative lateral positions across the width of the combined sprays (positions A, B, and C). These correspond to those located directly at the centerline of the combined sprays ($x = 0$ mm), almost directly below the axis of the needle of one of the sprays ($x = 4$ mm) and at the lateral periphery of that needle's spray ($x = 28$ mm), respectively, where x denotes the lateral (horizontal) distance from the centerline between the two needles and z is the axial (vertical) distance from the needles' tips.

As shown in Fig. 2, the axial velocity distribution having the greatest magnitude occurs directly below the axial center of the combined sprays. The magnitudes of the other axial distributions decrease in the direction lateral from this location. The lateral velocity distribution at position A is centered about a mean value of zero, with a slight asymmetry resulting from droplets centered about a mean value of approximately 1.0 m/sec. The magnitudes of the other lateral distributions become more negative in the direction lateral from this location. The droplet diameter distributions are unimodal, with the largest number of smallest diameter droplets occurring below a needle's centerline.

Information on droplet interspray mixing at this position can be obtained by examining the correlations between both the axial and lateral velocity components and droplet diameter, as shown in Figs. 3 and 4, respectively. In these figures, the outer region, bounded by a solid line, indicates the region(s) in which two or more correlations occurred for each velocity component and diameter pair measured. The inner, shaded region denotes where the majority of the droplet population resided, in which ten or more correlations occurred for each velocity component and diameter pair measured within the region.

The axial velocity component versus diameter correlation diagram for position A (Fig. 3) reveals that most of

 0899-8213/91/030492-03$02.00

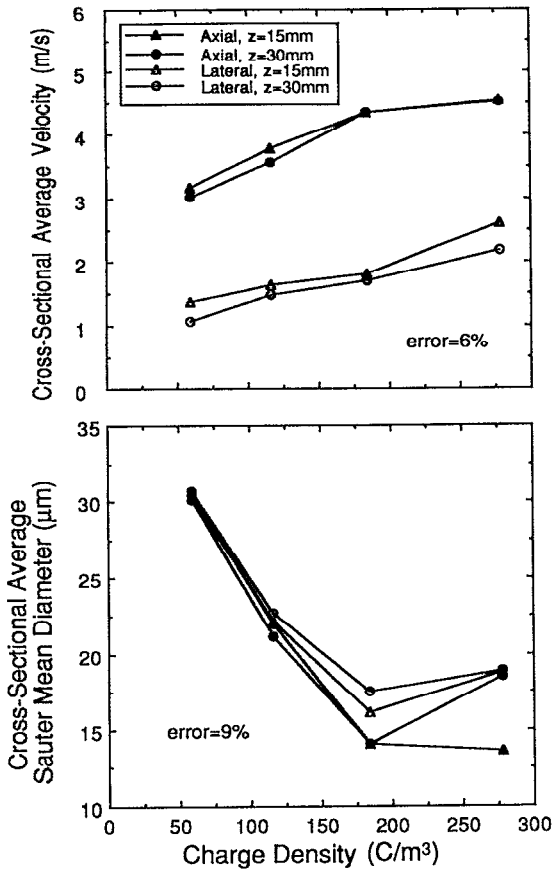

FIG. 1. Cross-sectional average values for each mean velocity component and Sauter mean diameter profile as a function of spray charge density (3 cm interneedle spacing).

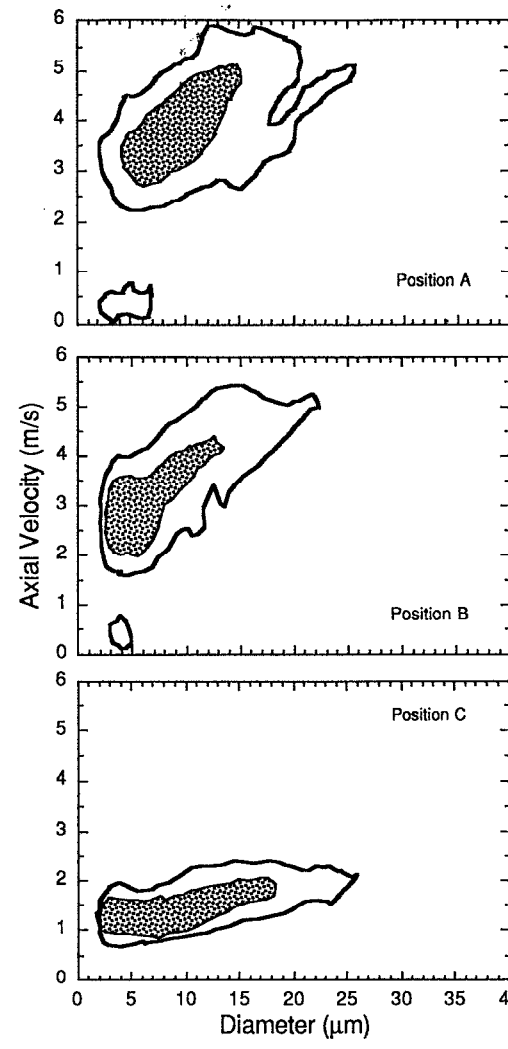

FIG. 3. Droplet axial velocity-component–diameter correlation diagrams, for positions A, B, and C, 1 cm interneedle spacing, 15 mm axial location, and 278 C/m^3.

the droplets are contained within one region. The corresponding lateral velocity component versus diameter correlation diagram (Fig. 4), however, shows a bifurcation of the outer region at approximately 22 μm, beyond which two distinct regions are present. The presence of these distinct regions for the same droplet diameter strongly suggests that the droplets from both sprays intermix at this location. At this symmetric, center location, if such mixing occurred, then the droplet axial component values would be of the same sign and magnitude and the lateral component values would be of the opposite sign but same magnitude. This is what is observed experimentally, particularly where the two regions are distinct. On the contrary, if the droplets were repelled at the midplane between the two sprays, there would be a continuum of lateral velocity component values and not distinct regions for the same droplet diameter. This clearly is not the case for the larger diameters ($d_d \gtrsim \sim 22\,\mu$m). Admittedly, however, for the smaller droplet diameters ($d_d \gtrsim \sim 22\,\mu$m), the distinction between droplet interspray mixing or repulsion cannot be made because of the resolution of the data in its present format.

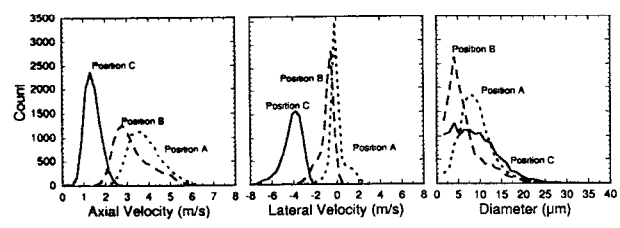

FIG. 2. Droplet axial and lateral velocity component and diameter distributions for positions A, B, and C, 1 cm interneedle spacing, 15 mm axial location, and 278 C/m^3.

In the regions directly below the axis of each of the two needles, the extent of this droplet interspray mixing is less. Both of the velocity component versus diameter correlations for position B, shown in Figs. 3 and 4, support that this results from a decrease in the number of droplets from one population and an increase in the other. This is a direct consequence of moving laterally away from the spray of one of the needles and more into the other. The two velocity component versus diameter correlation diagrams for this location, shown in Figs. 3 and 4, support that only the droplets from one needle contribute to the corresponding velocity component distribution.

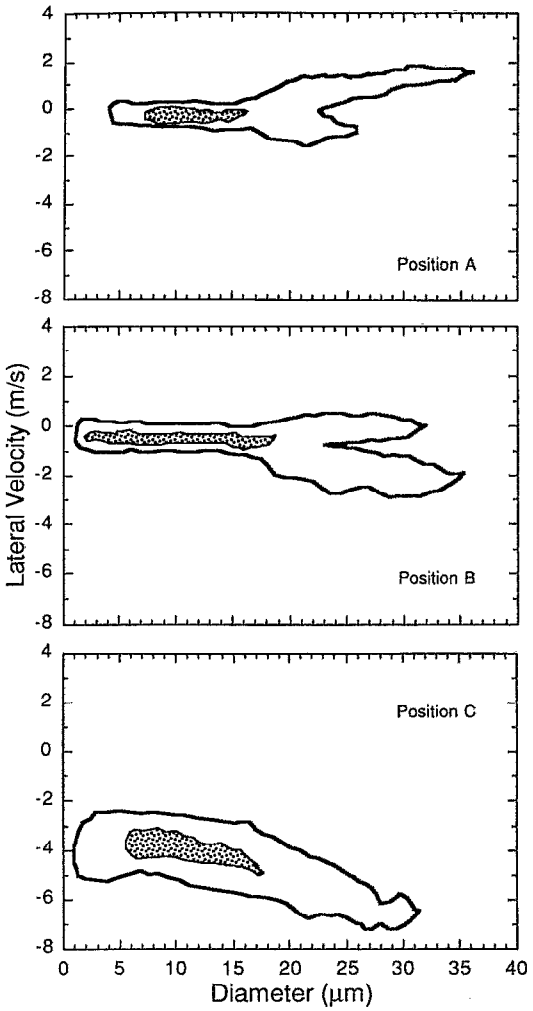

FIG. 4. Droplet lateral velocity-component–diameter correlation diagrams, for positions A, B, and C, 1 cm interneedle spacing, 15 mm axial location, and 278 C/m^3.

The correlation between velocity component and diameter can be examined in further detail. Because the motion of the droplets within the subject region are governed predominantly by the electric forces (Snarski and Dunn[2]), the governing equation of motion for a droplet reveals that its velocity equals the product of its electrical mobility, Z, and the strength of the composite electric field, $\bar{E}$, which is comprised of two terms: one from the externally imposed electric field, which is independent of q_d (the droplet charge), and the other from the electric field that arises from the presence of the charged droplets within the sprays, which is linearly related to q_d. Here, Z equals $q_d/3\pi\mu_m d_d$ (assuming Stokesian drag), where d_d is the droplet diameter and μ_m is the medium (air) absolute viscosity.

The droplet's velocity can be expressed in terms of its diameter by relating the droplet's electrical charge contained in both Z and $\bar{E}$ to the droplet diameter through the choice of the appropriate theory that describes the droplet charging process. If the liquid droplets are charged to their maximum (Rayleigh) limit, then q_d is proportional to $d_d^{3/2}$. If they have achieved a state of maximum entropy, then q_d is proportional to d_d, according to Kelly's equilibrium theory of droplet sprays.[4] This imples that the droplet velocity dependencies on diameter could range in the present experiments from none (assuming maximum entropy limit charging at the center) to d_d^2 (assuming Rayleigh limit charging at the periphery).

Examination of the 16 axial component velocity versus diameter correlations obtained at this interneedle spacing at the 15 mm axial location revealed a slight decrease in the value of the power of d_d with increasing lateral distance from the centerline of the combined sprays (from 0.46 to 0.16). Here, an average value equal to 0.33 with a standard deviation of 0.10 best described the observed behavior. The corresponding lateral component velocity versus diameter correlations showed no discernible dependency in the power of d_d upon lateral position and were best described by an average value equal to 0.40 with a standard deviation of 0.18. Such values of the power of d_d in these correlations support that Kelly's theory most closely models the observed behavior.

The results obtained at the 30 mm axial location revealed similar but less pronounced behavior. The lateral velocity-component–diameter correlation diagrams showed two distinct regions for the same diameter, but only at position A. Here, the value of the power of d_d was small ($\sim$0.10). This reduction in the correlation probably resulted from the decreased magnitude of the electric field contribution from the droplets that occurred as the interdroplet spacing increased and the spray broadened.

At an interneedle spacing of 3 cm, the results obtained at the 15 mm axial location showed no discernible bimodalities or velocity-component–diameter correlations. This was because, at this location and interneedle spacing, the two sprays were still somewhat distinct individual sprays that had not mixed. This finding implicitly suggests that the velocity component and diameter distributions of individual sprays at this charge density level are unimodal and have a negligible correlation between velocity component and diameter. The results obtained at the 30 mm axial location, however, were very similar to those obtained at the 15 mm axial location and 1 cm spacing. This supported that the increased interneedle spacing effectively moved the mixing region of the sprays farther downstream, which was consistent with the results reported previously by Snarski and Dunn.[2]

ACKNOWLEDGMENTS

We gratefully acknowledge the technical advice of Dr. V. J. Novick and Dr. E. D. Doss within the Engineering Physics Division of Argonne National Laboratory.

This work was performed under MIPR No. FY76168800343 between the University of Chicago and the Department of Defense and under Contract No. 62622401 between Argonne National Laboratory and the University of Notre Dame.

[1] A. J. Kelly, IEEE Trans. Ind. Appl. IA-20, 267 (1984).
[2] S. R. Snarski and P. F. Dunn, Particle Dynamics Laboratory Report No. UND/AME/PDL/SRS/PFD-89-1, University of Notre Dame, 1989 (to appear in Exp. Fluids).
[3] W. D. Bachalo and M. J. Houser, Opt. Eng. 23, 583 (1984).
[4] A. J. Kelly, J. Appl. Phys. 47, 5264 (1976).